Journal of Biomedical Optics

BiomedicalOptics.SPIEDigitalLibrary.org

Comprehensive vascular imaging using optical coherence tomography-based angiography and photoacoustic tomography

Behrooz Zabihian
Zhe Chen
Elisabet Rank
Christoph Sinz
Marco Bonesi
Harald Sattmann
Jason Ensher
Michael P. Minneman
Erich Hoover
Jessika Weingast
Laurin Ginner
Rainer Leitgeb
Harald Kittler
Edward Zhang
Paul Beard
Wolfgang Drexler
Mengyang Liu

Behrooz Zabihian, Zhe Chen, Elisabet Rank, Christoph Sinz, Marco Bonesi, Harald Sattmann, Jason Ensher, Michael P. Minneman, Erich Hoover, Jessika Weingast, Laurin Ginner, Rainer Leitgeb, Harald Kittler, Edward Zhang, Paul Beard, Wolfgang Drexler, Mengyang Liu, "Comprehensive vascular imaging using optical coherence tomography-based angiography and photoacoustic tomography," *J. Biomed. Opt.* **21**(9), 096011 (2016), doi: 10.1117/1.JBO.21.9.096011.

SPIE.

Comprehensive vascular imaging using optical coherence tomography-based angiography and photoacoustic tomography

Behrooz Zabihian,[a] Zhe Chen,[a] Elisabet Rank,[a] Christoph Sinz,[b] Marco Bonesi,[a] Harald Sattmann,[a] Jason Ensher,[c] Michael P. Minneman,[c] Erich Hoover,[c] Jessika Weingast,[b] Laurin Ginner,[a] Rainer Leitgeb,[a] Harald Kittler,[b] Edward Zhang,[d] Paul Beard,[d] Wolfgang Drexler,[a,*] and Mengyang Liu[a]

[a]Medical University of Vienna, Center for Medical Physics and Biomedical Engineering, AKH 4L, Währinger Gürtel 18-20, Vienna 1090, Austria
[b]Medical University of Vienna, Department of Dermatology, Währinger Gürtel 18-20, Vienna 1090, Austria
[c]Insight Photonic Solutions, Inc., 300 South Public Road, Lafayette, Colorado 80026, United States
[d]University College London, Department of Medical Physics and Biomedical Engineering, Gower Street, London, United Kingdom

Abstract. Studies have proven the relationship between cutaneous vasculature abnormalities and dermatological disorders, but to image vasculature noninvasively *in vivo*, advanced optical imaging techniques are required. In this study, we imaged a palm of a healthy volunteer and three subjects with cutaneous abnormalities with photoacoustic tomography (PAT) and optical coherence tomography with angiography extension (OCTA). Capillaries in the papillary dermis that are too small to be discerned with PAT are visualized with OCTA. From our results, we speculate that the PA signal from the palm is mostly from hemoglobin in capillaries rather than melanin, knowing that melanin concentration in volar skin is significantly smaller than that in other areas of the skin. We present for the first time OCTA images of capillaries along with the PAT images of the deeper vessels, demonstrating the complementary effective imaging depth range and the visualization capabilities of PAT and OCTA for imaging human skin *in vivo*. The proposed imaging system in this study could significantly improve treatment monitoring of dermatological diseases associated with cutaneous vasculature abnormalities. [DOI: 10.1117/1.JBO.21.9.096011]

Keywords: photoacoustic tomography; optical coherence tomography; angiography; human skin; capillary; papillary dermis.

Paper 160354LRR received Jun. 3, 2016; accepted for publication Aug. 29, 2016; published online Sep. 22, 2016.

The epidermis is the outermost layer of skin. Volar skin is characterized histologically by a thick cornified layer and a prominent undulate pattern of epidermal rete ridges and dermal papillae, which ensure a tight junction of the epidermis and the dermis.[1] The superficial vascular plexus consists of a network of vessels that are parallel to the skin surface. Hairpin-shaped capillaries from vessels of the superficial plexus loop into the dermal papillae.[1] Through the permeable wall of capillaries metabolic substances are delivered to and transported from the avascular epidermis.[2]

The vasculature of the superficial plexus and especially post-capillary venules are the principal sites of pathologic changes in most inflammatory skin diseases.[3] For instance, abnormalities in these vessels have significant and active impact on pathogenesis of psoriasis[4] which is characterized by tortuous and dilated vessels in the papillary dermis.[5] During remission after photochemotheraphy with oral psoralen, psoriasis lesions exhibit shortening of capillary loops due to reversion from venous capillary to arterial capillary.[6] Videocapillaroscopy and dermatoscopy have been used successfully to monitor treatment effects because the morphologic changes of capillaries in the papillary dermis mirror the evolution and involution of psoriasis plaques during and after therapy.[7,8]

Archid et al.[7] reported confocal laser-scanning microscopy (CLSM) of capillaries. CLSM has a high axial resolution of 5 μm and a lateral resolution between 1 and 3 μm. However, it has limited penetration and low sensitivity to blood particles and therefore is not suitable for imaging capillaries in the dermis. Photoacoustic maging (PAI), based on optical absorption of light, has superb sensitivity to hemoglobin in red blood cells.[9] Optical-resolution photoacoustic microscopy (OR-PAM) uses a focused beam for excitation and provides high resolution with the tradeoff of imaging depth, whereas photoacoustic tomography (PAT) uses a diffused excitation beam and has deeper imaging depth.[9] A recent publication[10] demonstrated the capabilities of a dual-modality PAT/optical coherence tomography (OCT) system in imaging various dermatological diseases. Benefiting from the light absorption properties of blood and structural deformation due to dermatological lesions, several abnormalities were imaged. The reported system visualized major blood vessels. Several other studies have shown vascular network in volar skin using PAI,[11–13] but most of them use piezoelectric transducers and lack the sensitivity to adequately visualize the capillaries in the papillary dermis. This shortcoming in discerning the finer capillaries in the papillary dermis motivates the current study.

Van Es et al.[13] reported a finger imaging PAT system and presented images from a healthy volunteer. The system could detect PA signals from the capillaries in the dermal papillae but could not visualize the capillary network. Aguirre et al.[12] utilized a broadband ultrasound transducer and presented PAT

*Address all correspondence to: Wolfgang Drexler, E-mail: wolfgang.drexler@meduniwien.ac.at

images of the collection of capillaries in the papillary dermis. However, their systems were incapable of visualizing individual capillaries.

OCT-based angiography (OCTA) is an extension of OCT that can easily visualize vascular structure down to the level of capillaries in human skin.[11,14–16] The contrast in OCTA is based on moving scatterers in blood.[17] The high lateral resolution and deep imaging depth make OCTA a strong competitor to PAM when it comes to imaging capillaries in skin. Especially when we notice that in spite of the success of OR-PAM in vasculature imaging preclinically, to the authors' knowledge, it has not been demonstrated clinically in human skin imaging, which could be attributed to the current configurations of standard OR-PAM being not optimal for *in vivo* clinical applications.

A particular advantage of OCTA is the short imaging time, which permits *in vivo* applications in a much faster manner. Stepper motor-based PAM systems do not meet the critical time requirement in many preclinical and clinical applications. Fast PAM systems were proposed but all have limitations for certain dermatological applications. Fast laser-scanning OR-PAM can achieve high imaging speed, but its scanning range is usually about 200 μm laterally.[18] Increasing the size of an unfocused transducer to increase the scanning range has the drawback of passively increasing the amplifier input load of the transducer.[18] A water-immersible microelectromechanical systems (MEMS)-based setup was reported.[19] With a volumetric scan rate of 0.8 Hz, i.e., 20 times faster than a voice-coil-based system, its scanned area was limited to 2 mm × 5 mm. In contrast, OCTA can cover an area of 10 mm × 10 mm in just a few seconds. Besides, OCTA as an extension for OCT can provide morphological information simultaneously, and the significance of OCT revealed morphology in dermatological studies has been proven in Ref. 20.

In this letter, we demonstrate for the first time the advantage of using OCTA in imaging the finer capillaries in the shallower depth and the major blood vessels in the deeper dermis using PAT. Both phase-based and intensity-based angiography are achieved using this OCTA system. Details of the system and its algorithm can be found in Ref. 21. The light source was centered at 1310 nm (SSOCT-1310 Insight Photonic Solutions, Inc.) with a bandwidth of 37 nm and a sweep rate of 200 kHz. The lateral and axial resolutions of the system were 45 and 26 μm, respectively. The sensitivity of the OCTA system was measured to be 103 dB. The schematic of the PAT system is given in Ref. 10.

In this study, one healthy subject and three subjects with cutaneous abnormalities were imaged. This study was approved by the ethics committee of the Medical University of Vienna and followed the Declaration of Helsinki. For the healthy subject, skin on top of the thenar eminence area of the palm was imaged with PAT and then with OCTA. The scanned area for PAT was 14.16 mm × 14.16 mm for all the subjects and for OCTA it was 8 mm × 8 mm for the healthy subject and 10 mm × 10 mm for the rest. The total acquisition time was 4.6 min for PAT and about 30 s for OCTA. The number of A-scans and B-scans for OCTA were 512 and 512, respectively. A square was drawn

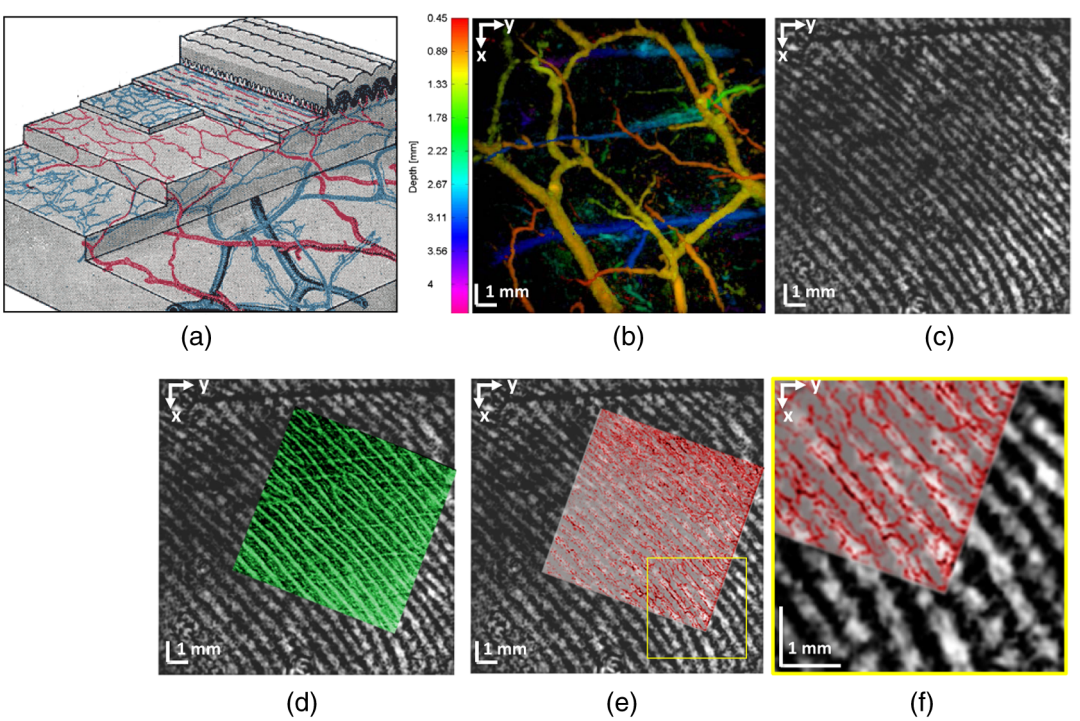

Fig. 1 (a) Diagram of vasculature in volar skin adapted from Ref. 22.(b) Color-coded MIP PAT of healthy skin covering the depth range from 0.45 to 4.44 mm. (c) MIP PAT covering the depth range between 0.27 and 0.42 mm. The bright parallel curves depict the superficial vascular plexus and capillary loops within each ridge. (d) Overlay of the PAT in (c) with structural OCT (green color map) covering the same depth range. The bright curves are the epidermal projections that follow the furrows and in between two adjacent projections are the ridges. (e) Overlay of the PAT in (c) with OCTA (red color map) integrating the same depth range. (f) Zoomed in view of the yellow square in (e) showing the superficial vascular plexus that runs parallel to the skin surface at the edge of each ridge. The capillary loops that are composed of finer arterial and venous capillaries are connected to the major capillaries inside each ridge.

using a marker on the skin to indicate the region to be scanned for both modalities.

Figure 1(a) is a diagram of the vascular network in human volar skin.[22] Notice the dermatoglyphic pattern of ridges and furrows on the surface of the skin and the parallel vessels of the superficial vascular plexus just below the epidermis. Figures 1(b) and 1(c) show the PAT and Figs. 1(d)–(f) show OCT overlaid on PAT images. These figures are maximum intensity projection (MIP) images in the depth direction. Figure 1(b) is a depth-color coded MIP image integrating the depth range from 0.45 to 4.44 mm; the color bar to the left of the figure depicts the corresponding depth in millimeters for hue. This figure shows major vessels located in the reticular dermis and upper part of the subcutis. Figure 1(c) is MIP PAT image of the capillaries in the papillary dermis, covering the depth range from 0.27 to 0.42 mm. In Fig. 1(d), the green color map is structural OCT, integrating the same depth range as the PAT image. The bright curves are the epidermal projections that follow the furrows and the darker bands between them are the ridges. This figure demonstrates the coregistration of data from the two modalities. Figure 1(e) is an overlaid OCTA image (red color map) on the PAT image. Figure 1(f) is a zoomed in image of the yellow square in Fig. 1(e). In Fig. 1(e), the OCTA image reveals finer vessels that are not discernable by PAT. Between two dermal papillae there is a downward projection of the epidermis called crista intermedia, which is situated below the center of the ridges. In the periphery, the dermal papillae are flanked by two epidermal projections that follow the furrows. The vasculature that runs parallel to the skin surface consists of the arterioles of the superficial vascular plexus. The capillary loops in the dermal papilla are composed of an ascending arterial component and a descending venous limb. The venous portion of a capillary loop empties into postcapillary venules of the superficial plexus. The capillaries deliver oxygen and nutrition to the epidermis, which is devoid of vessels.[6] The diameter of individual capillary is too small to be discerned with PAT, but the superficial vascular plexus can be discerned. The OCTA image, on the other hand is capable of resolving smaller vessels. In the OCTA image in Fig. 1(f), the vessels of the superficial plexus run at the edge of each ridge. The network of capillary loops within each ridge, connected to the larger ones are barely visible as small dots.

The same area imaged with PAT/OCTA was imaged with confocal microscopy after the experiment. The confocal microscopy images detected melanin in the lower part of the epidermis, i.e., stratum Malpighii. The melanin could contribute to the PA signal that is visualized in Figs. 1(c)–1(f). However, it is known that melanin content of volar skin is relatively low, significantly less than other parts of the skin.[23] On the other hand, the capillary loops in the dermal papillae are located underneath the ridges and the vessels of the superficial vascular plexus run along the ridges. The MIP PAT image of these vessels is confined to the pattern of the ridges. The coregistered PAT and OCT images suggest that parallel lines of Fig. 1(c) correspond to the ridges and therefore we believe that the parallel lines in the PAT images mostly represent hemoglobin and not melanin.

Figure 2(a) shows the MIP PAT image integrating the depth range between 0.45 and 1.01 mm. Figure 2(b) shows the overlaid OCTA image. Figure 2(b) shows the maximum effective imaging depth of OCTA in a human palm. Figure 2(c) shows a single frame from the three-dimensional (3-D) rendered video of the coregistered PAT and OCTA data.

Nevus araneus is a benign vascular lesion that can be associated with pregnancy, extra estrogen, or poor liver function. It is distinguished by a central papule and a network of feeding capillaries with a radial pattern. Figure 3 shows the results acquired by imaging a subject with nevus araneus on the dorsum of the hand. Figure 3(a) is a depth-color coded MIP image integrating the depth range from 0.64 to 3.00 mm. Figure 3(b) is an MIP PAT image integrating the depth range from 623 to 940 μm. In Fig. 3(c), the OCTA image of the corresponding depth range is overlaid on the PAT image of Fig. 3(b), showing the depth overlap of the two modalities. The corresponding blood vessels in the two modalities are marked with yellow arrows 1 and 2. Figure 3(d) is the OCTA integrating the depth range from 221 to 389 μm. This figure shows the finer vessels that are not discernible using PAT. Figure 3(e) is 3-D rendering of the three modalities. OCT shows skin morphology in gray color map, OCTA in red, and PAT in golden. Figure 3(f) is a photograph of the imaged site.

Cherry angioma manifests itself with benign dilation of blood vessels or proliferation of endothelial cells. They are often single or multiple small, cherry red papules. Figure 4 shows the results of imaging cherry angioma on an upper arm *in vivo*. Figure 4(a) is a depth-color coded MIP image integrating the depth range from 380 to 2350 μm. Figures 4(b) and 4(c) are PAT and OCTA overlaid on pat, respectively. Figure 4(d) is an MIP PAT image integrating the depth range from 20 to 110 μm. In this image, the angioma is seen as a bright spot in the top region of the image. Figures 4(e) and 4(f) are OCTA

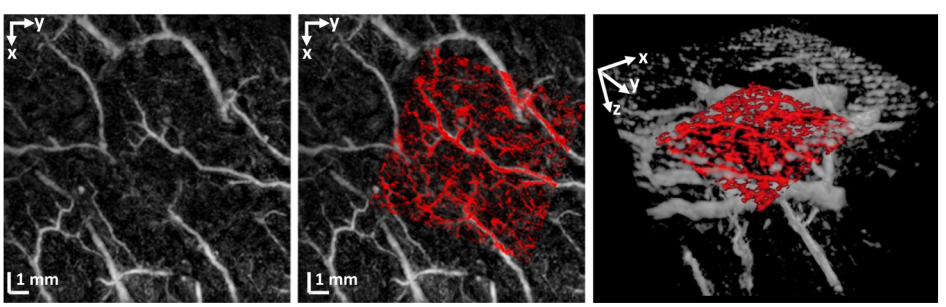

(a) (b) (c)

Fig. 2 (a) PAT and (b) OCTA overlaid on PAT images of the vascular network in the dermis, integrating the depth range between 0.45 and 1.01 mm. The red colormap corresponds to the OCTA data. (c) Single frame from the 3-D-rendered video of fused PAT and OCTA. The video is provided in the supplementary material (Video 1, mov, 10.9 MB) [URL: http://dx.doi.org/10.1117/1.JBO.21.9.096011.1].

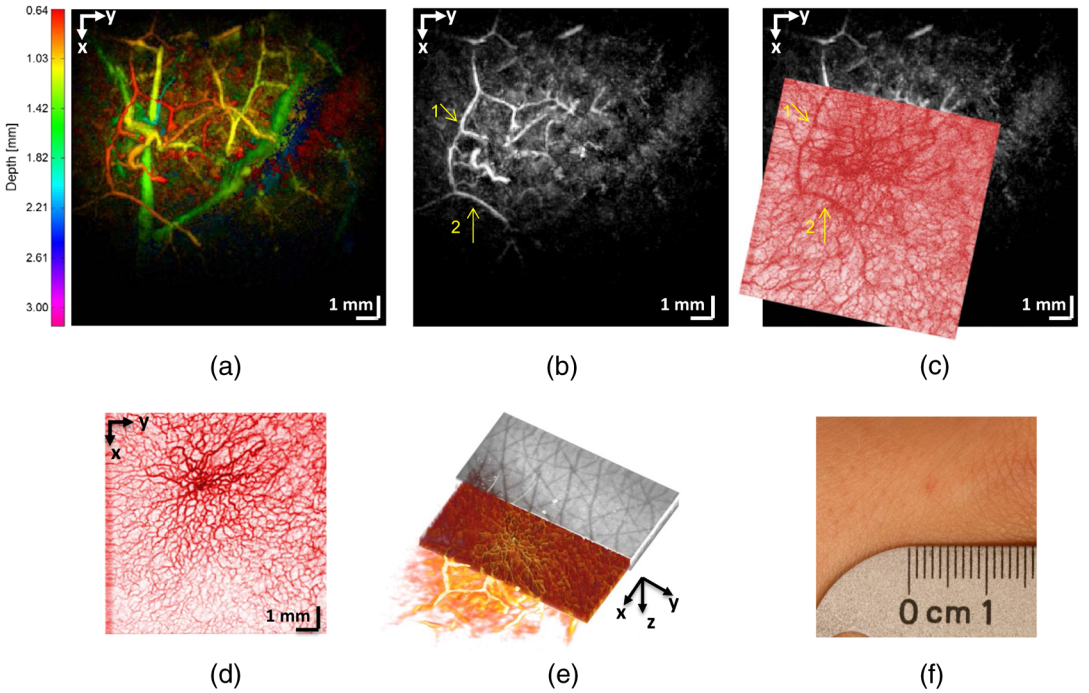

Fig. 3 Nevus araneus on dorsum of hand. (a) Depth-color coded MIP PAT image. (b) An MIP PAT image integrating the depth range from 623 to 940 μm and (c) overlaid OCTA of corresponding depth on it. The common vessels seen by both PAT and OCTA are marked with yellow arrows 1 and 2. (d) OCTA showing the finer capillaries that feed the central arteriole at the depth range from 221 to 389 μm. These capillaries are not discernible by PAT. (e) 3-D rendered fusion of the three modalities: OCT showing skin morphology with gray color map, OCTA with red and PAT with golden. (f) Photograph of the imaged site.

images; Fig. 4(e) is a cross sectional image. In this image, the green and blue lines indicate the depth where the *en face* images in Fig. 4(f) are obtained and the red line corresponds to the OCTA image in Fig. 4(c). By comparing Figs. 4(d) with 4(b), we can see that the abnormality exists only on the surface of the skin and does not span in depth. The feature seen in *en face* OCTA images in depth, e.g., Fig. 4(f) is due to a shadowing artifact in OCTA. Figure 4(g) is a photograph of the imaged site on the upper arm of the subject.

Figure 5 shows the results of imaging an upper dermis angioma located on the upper leg of a human subject. Clinical image shows a flat blue lesion. Figure 5(a) shows a depth-color coded MIP PAT image integrating the depth range from 380 to 1500 μm. The angioma is seen as a bright oval spot roughly in the center of the image at the depth of ~500 μm below skin surface. Figures 5(b) and 5(c) are images of PAT and OCTA overlaid on PAT, respectively. In these figures, the vessels that are visualized by both modalities are marked with yellow arrows from 1 to 3. While OCTA is capable of discerning dense mesh of finer vessels in the area of the angioma, in PAT this mesh is visualized featuring an oval shape. Figure 5(d) is the OCTA showing a depth range from 364 to 390 μm. Figure 5(e) is the photograph of the imaged site.

A broad variety of dermatologic diseases leads to microangiopathic changes. OCTA applied to skin showed characteristic patterns for skin pathologies such as basal cell carcinoma or psoriasis.[16] In addition to inflammatory diseases such as cutaneous vasculitis, autoimmune disorders like Raynaud's phenomenon or connective tissue diseases are also associated with microvascular changes.[24] Diabetes mellitus, a very common metabolic disorder, affects the vasculature of skin and leads to microangiopathy[25] which affects the dermal blood flow and leads to skin ulcerations and impaired wound healing.[26]

OCT can provide structural information and visualize morphological changes in skin. OCTA enables label free visualization of small vessels and is complementary to PAT. An axial range with effective blood vessel visualization for OCTA was found to be about 996 μm. Although the current scan lens (Thorlabs, LSM04 with center wavelength of 1315 nm and a mean spot size of 35 μm) does not permit fine lateral resolution comparable to the diameter of capillary loops, as long as the decorrelation caused by capillary blood flow passes the lower threshold in the reconstruction algorithm, the microvasculature can still be visualized with broadened diameter.[27] In the literature, the diameter of capillaries is 4 to 8 μm and 10 to 30 μm for postcapillary venules.[1] This artificial broadening of microvasculature was measured to be roughly six times for capillaries and three times for postcapillary venules. PAT and OCTA together can reveal the overall vascular network. Here we showed how OCTA is capable of visualizing the superficial vascular plexus and the capillaries in the papillary dermis. We also showed the depth-range overlap of PAT and OCTA. In Fig. 4, results of imaging cherry angioma were presented. This abnormality was at the surface of skin. A drawback of OCTA is a shadow artifact of vessels. In *en face* images of OCTA at different depths, we can see the identical spot that is the shadow of the angioma at the surface. On the other hand, PAT is more resilient to a shadow artifact. The PAT image of deeper depth in Fig. 4(b) confirms that the angioma does not have depth profile.

Even though the PAT/OCT combined system has been demonstrated for clinical use previously,[10] phased-based angiography was not possible with the previous system. This work

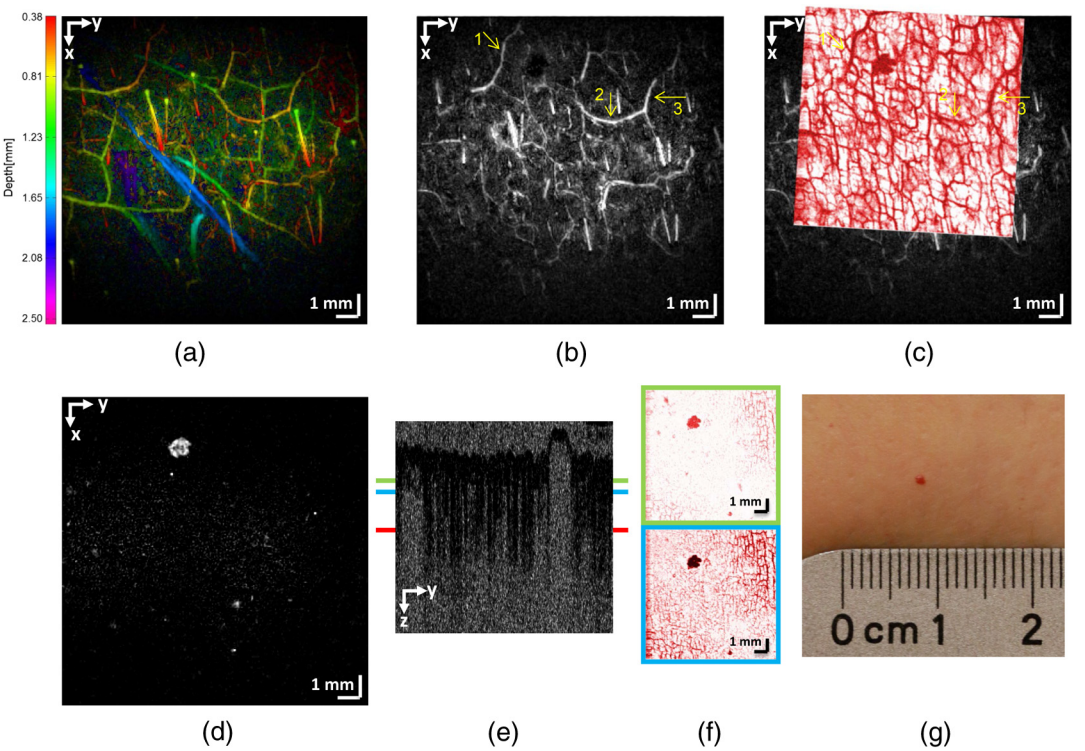

Fig. 4 Cherry angioma on upper arm. (a) Depth-color coded MIP PAT image showing vessels up 2.3 mm in depth. (b) and (d) MIP PAT images integrating the depth range 380 to 760 μm and 20 to 110 μm, respectively. (c) OCTA overlaid on PAT from (b). (e) Cross-sectional image of OCTA; the green and blue horizontal lines show the depth where the *en face* images in (f) are taken from. The red line indicates the depth corresponding to the OCTA in (c). The lesion is at the surface of the skin and it causes shadow artifact in OCTA at deeper depth, i.e., the spots in (f). By comparing the PAT in (b) and (d), we can see that the lesion is indeed not visible in depth; i.e., the white bright spot seen in (d) is not visible in (b). (g) Photograph of the imaged site.

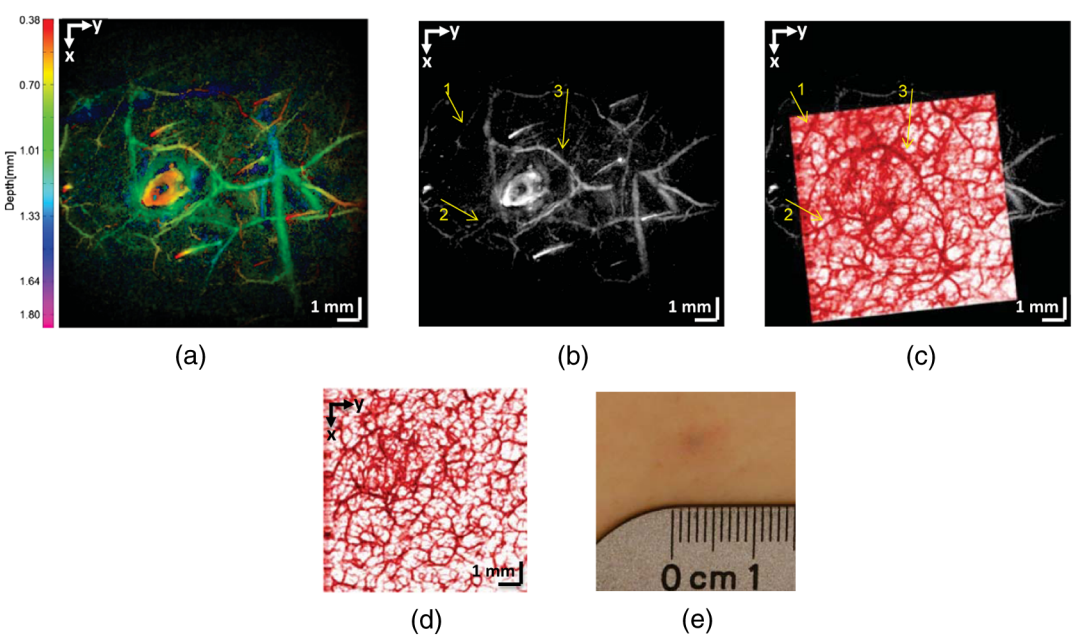

Fig. 5 Angioma of upper dermis in upper leg. (a) Color-coded MIP PAT, the lesion is seen as an oval shape roughly in the center of the image. (b) and (c) MIP PAT integrating depth range from 380 to 990 μm and overlaid OCTA. The corresponding vessels in PAT and OCTA are marked with yellow arrows 1 to 3. (d) OCTA integrating depth range from 364 to 390 μm. Note the dens capillaries in the lesion area. The lesion area is in between arrows 2 and 3 in (c). (e) Photograph of the imaged site.

proves the potential to use a phase stable akinetic swept source OCT for microvasculature visualization, which initiates our future work to design a trimodality combined PAT/OCT/OCTA system for human skin vasculature imaging.

To the best of our knowledge, we presented here for the first time *in vivo* images of the capillaries of human palm with great details using OCTA along with the larger vessels of deeper depth using PAT. In the near future, this may help provide valuable information for microvascular perfusion which can thereon enable a noninvasive and fast assessment for a spectrum of skin diseases with vascular malformation.

Acknowledgments

We acknowledge the help of C. Glittenberg. This project was funded by Interdisciplinary Coupled Physics Imaging (Project No. P26687-N25) and the European project FAMOS (Project No. FP7 ICT 317744).

References

1. S. Standring, *Gray's Anatomy, the Anatomical Basics of Clinical Practice*, Elsevier, Edinburgh (2005).
2. P. McKee, *Pathology of the Skin with Clinical Correlations*, Mosby-Wolfe, London (1996).
3. R. Huggenberger and M. Detmar, "The cutaneous vascular system in chronic skin inflamation," *J. Invest. Dermatol. Symp. Proc.* **15**(1), 24–32 (2011).
4. G. Micali et al., "Cutaneous vascular patterns in psoriasis," *Int. J. Dermatol.* **49**(3), 249–256 (2010).
5. S. P. Barton, M. S. Abdullah, and R. Marks, "Qualification of microvascular changes in the skin in patients with psoriasis," *Br. J. Dermatol.* **126**(6), 569–574 (1992).
6. I. M. Braverman, "The cutaneous microcirculation," *J. Invest. Dermatol. Symp. Proc.* **5**(1), 3–9 (2000).
7. R. Archid et al., "Confocal laser-scanning microscopy of capillaries in normal and psoriatic skin," *J. Biomed. Opt.* **17**(10), 101511 (2012).
8. P. Rosina et al., "Microcirculatory modifications of psoriatic lesions during topical therapy," *Skin Res. Technol.* **15**(2), 135–138 (2009).
9. J. Yao and L. V. Wang, "Photoacoustic tomography: fundamentals, advances and prospects," *Contrast Media Mol. Imaging* **6**(5), 332–345 (2011).
10. B. Zabihian et al., "In vivo dual-modality photoacoustic and optical coherence tomography imaging of human dermatological pathologies," *Biomed. Opt. Express* **6**(9), 3163–3178 (2015).
11. C. P. Favazza, L. A. Cornelius, and L. V. Wang, "*In vivo* functional photoacoustic microscopy of cutaneous microvasculature in human skin," *J. Biomed. Opt.* **16**(2), 026004, (2011).
12. J. Aguirre et al., "Broadband mesoscopic optoacoustic tomography reveals skin layers," *Opt. Lett.* **39**(21), 6297–6300 (2014).
13. P. van Es et al., "Initial results of finger imaging using photoacoustic computed tomography," *J. Biomed. Opt.* **19**(6), 060501 (2014).
14. Z. Zhi et al., "4D optical coherence tomography-based micro-angiography achieved by 1.6-MHz FDML swept source," *Opt. Lett.* **40**(8), 1779–1782 (2015).
15. W. Drexler et al., "Optical coherence tomography today: speed, contrast, and multimodality," *J. Biomed. Opt.* **19**(7), 071412 (2014).
16. C. Blatter et al., "In situ structural and microangiographic assessment of human skin lesions with high-speed OCT," *Biomed. Opt. Express* **3**(10), 2636–2646 (2012).
17. L. An, J. Qin,, and R. K. Wang, "Ultrahigh sensitive optical microangiography for in vivo imaging of microcirculations within human skin tissue beds," *Opt. Express* **18**(8), 8220–8228 (2010).
18. C. Yeh et al., "Three-dimensional arbitrary trajectory scanning photoacoustic microscopy," *J. Biophotonics* **8**(4), 303–308 (2015).
19. J. Yao et al., "Wide-field fast-scanning photoacoustic microscopy based on a water-immersible MEMS scanning mirror," *J. Biomed. Opt.* **17**(8), 080505 (2012).
20. A. Alex et al., "Three-dimensional multiphoton/optical coherence tomography for diagnostic applications in dermatology," *J. Biophotonics* **6**(4), 352–362 (2013).
21. Z. Chen et al., "Phase-stable swept source OCT angiography in human skin using an akinetic source," *Biomed. Opt. Express* **7**(8), 3032–3048 (2016).
22. H. Gray, *Anatomy of the Human Body*, 24th ed., Lea & Febiger, Philadelphia (1944).
23. Y. Yamaguchi et al., "Mesenchymal-epithelial interactions in the skin: increased expression of dickkopf1 by palmoplantar fibroblasts inhibits melanocyte growth and differentiation," *J. Cell Biol.* **162**(2), 275–285 (2004).
24. C. Griffiths et al., *Rook's Textbook of Dermatology*, 8th ed., Wiley-Blackwell, Oxford (2010).
25. A. C. Huntley, "Cutaneous manifestation of diabetes mellitus," *Dermatol. Clin.* **7**(3), 531–546 (1989).
26. M. A. Loots et al., "Cultured fibroblasts from chronic diabetic wounds on the lower extremity show disturbed proliferation," *Arch. Deratol. Res.* **291**(2), 93–99 (1999).
27. M. Liu et al., "Combined multi-modal photoacoustic tomography, optical coherence tomography (OCT) and OCT angiography system with an articulated probe for in vivo human skin structure and vasculature imaging," *Biomed. Opt. Express* **7**(9), 3390–3402 (2016).

Behrooz Zabihian received his MSc degree in electronics and telecommunication from University of Algrave, Portugal. He is a doctoral student at Center for Medical Physics and Biomedical Engineering, Medical University of Vienna, Austria. During his doctoral studies, he worked on multimodal photoacoustic and optical coherence tomography for visualizing morphology and vasculature with clinical and preclinical applications. His interests include signal processing, instrumentation, and noninvasive medical imaging.

Zhe Chen received his master's degree in medical physics at Heidelberg University in 2014. He is a doctoral student at the Medical University of Vienna, Austria. His current main research interest is on the dual modality optical coherence tomography angiography (OCTA) and photoacoustics tomography (PAT) imaging technique. Furthermore, he also has interest in investigation of skin diseases with PAT-OCT-OCTA.

Elisabet Rank received her MSc degree in biomedical engineering from the University of Applied Sciences Technikum Wien, Austria. She is a PhD student at the Medical University of Vienna, Austria. Her research interests span from optical coherence tomography to photoacoustic tomography. Currently, she is developing novel optical coherence tomography systems as well as conducting clinical studies.

Christoph Sinz is doctor-in-training at the Department of Dermatology, Medical University of Vienna. His research interests are diagnostic imaging, early detection of skin-cancer and computer-assisted image interpretation.

Marco Bonesi earned his PhD from Cranfield University, United Kingdom, in 2008. The title of his PhD thesis was "Characterization of flow dynamics in vessels with complex geometry using Doppler optical coherence tomography." His research interests include optical engineering, electronic engineering, and biomedical engineering.

Harald Sattmann graduated from Technologische Gewerbemuseum in Vienna, Austria, in 1976. He then studied information technology at Technical University of Vienna. He is currently technical support for electronics at Center for Medical Physics and Biomedical Engineering at Medical University of Vienna, Austria.

Jason Ensher is the CTO and VP for strategic marketing at Insight Photonic Solutions, where he leads development of akinetic tunable lasers. He earned his PhD in atomic physics at the University of Colorado in Boulder, for the Nobel-winning creation of Bose-Einstein condensation. He is the author of 30 peer-reviewed papers and 19 patents. For the past 16 years he has developed lasers and opto-electronics in biomedical imaging and other fields.

Michael P. Minneman is the president and CEO at Insight Photonic Solutions and member of expert advisory team at Key Sensor

Photonics. He received his BSEE degree from the University of Washington in 1981 and his MBA degree from the same university in 1985. He co-authored several peer-reviewed papers and more than 20 patents.

Erich Hoover received his BSc degree in engineering physics in 2007, and his MSc degree in engineering with an electrical specialty in 2008, and his PhD in applied physics in 2012, from the Colorado School of Mines, Golden. Since 2013, he has worked for Insight Photonic Solutions improving their swept laser engine. His research interests include the application of hardware and software for controlling medical imaging technologies.

Jessika Weingast is a board-certified dermatologist and is currently completing her PhD thesis on the relevance of OCT as noninvasive diagnostic tool in nonmelanoma skin cancer.

Laurin Ginner graduated from the Francsico Josephinum Wieselburg. After graduation, he received his university bachelor's degree in technical physics and master's degree in physical energy and measurement engineering. He did diploma thesis in "Improvement of high speed swept source optical coherence tomography for optical angiography." Since 2015, he is a PhD student at the Medical University of Vienna in the topic of line field OCT and high-resolution imaging.

Rainer Leitgeb is a associate professor at the Medical University of Vienna since 2003, specializing in functional OCT, multimodal imaging, and advanced microscopy. Since 2015, he is head of the Christian Doppler Laboratory for Innovative Optical Imaging and its Translation to Medicine. From 2004 to 2007, he worked at the EPFL, Switzerland, as an invited professor. He has been awarded the ARVO/ALCON early career clinical scientist award and is a fellow of SPIE and OSA.

Harald Kittler holds the position of associate professor of dermatology at the Department of Dermatology at the Medical University of Vienna and leads the research team for *in-vivo* skin imaging. He graduated from Medical University in 1994 and completed his residency in dermatology in 2002. He received postgraduate training in dermatopathology at the Ackerman Academy in New York. He published more than 140 articles in peer-reviewed journals mainly on dermatoscopy and computer-assisted diagnosis.

Edward Zhang is a senior research fellow at the Department of Medical Physics and Biomedical Engineering at UCL. He received his PhD in 1994 from City University, United Kingdom. His interests are fiber optic sensor and fluorescence thermometry, optical fiber amplifiers and telecommunications, and photoacoustic technology for biomedical applications.

Paul Beard is a professor of biomedical photoacoustics at UCL. He founded and leads the Photoacoustic Imaging Group within the Department of Medical Physics and Bioengineering. The group's activities are directed towards the development of a new method of noninvasive biomedical imaging for visualizing the structure and function of soft tissues. Their research includes photoacoustic instrumentation, photoacoustic signal modelling, image reconstruction algorithms, spectroscopic methods and the application of the technique in the clinical and life sciences.

Wolfgang Drexler was a full professor of biomedical imaging at Cardiff University, United Kingdom, from 2006 to 2009. Since 2009, he is a full professor and the head of the Center for Medical Physics and Biomedical Engineering at the Medical University of Vienna, Austria. He spent two years at MIT; received the Austrian START Award (2001) and the COGAN Award (2007); published more than 180 papers; gave about 180 invited/keynote talks; and accomplished € 11 million research grant income.

Mengyang Liu received his MSc degree in electrical and computer engineering from the University of Delaware and his PhD degree in medical physics from the Medical University of Vienna. He is currently a university assistant at the Medical University of Vienna. His research interest includes photoacoustic imaging and optical coherence tomography with a main focus on the combination of these two optical imaging modalities for translational research.